IEEE Access
Multidisciplinary ⋮ Rapid Review ⋮ Open Access Journal

Received April 20, 2022, accepted May 15, 2022, date of publication May 20, 2022, date of current version June 3, 2022.

Digital Object Identifier 10.1109/ACCESS.2022.3176623

31 dBi-Gain Slotted Waveguide Antenna Array Using Wing-Based Reflectors

EVANDRO C. VILAS BOAS[1], MARCO A. S. FERRERO[1], ABDELKHALEK NASRI[2], RAJ MITTRA[2,3], (Life Fellow, IEEE), AND ARISMAR C. SODRÉ, JR.[1]

[1]Wireless and Optical Convergent Access (WOCA Laboratory), Department of Telecommunication Engineering, National Institute of Telecommunication (Inatel), Santa Rita do Sapucaí 37540-000, Brazil
[2]Department of Electrical and Computer Engineering, University of Central Florida, Orlando, FL 32816, USA
[3]Electrical and Computer Engineering Department, Faculty of Engineering, King Abdulaziz University, Jeddah 21589, Saudi Arabia

Corresponding author: Arismar C. Sodré, Jr. (arismar@inatel.br)

This work was supported in part by Rede Nacional de Ensino e Pesquisa (RNP) through Ministério da Ciência, Tecnologia, Inovações e Comunicações (MCTIC) under the Radiocommunication Reference Center (Centro de Referência em Radiocomunicações—CRR) Project of the National Institute of Telecommunications (Instituto Nacional de Telecomunicações—Inatel), Brazil, under Grant 01250.075413/2018-04; in part by the Coordenação de Aperfeiçoamento de Pessoal de Nível Superior—Brazil (CAPES)—Finance Code 001; in part by Conselho Nacional de Desenvolvimento Científico e Tecnológico (CNPq), Ministério da Ciência, Tecnologia e Inovações (MCTI), and Fundação de Amparo à Pesquisa do Estado de Minas Gerais (FAPEMIG); and in part by Keysight and Engineering Simulation and Scientific Software (ESSS)-ANSYS.

ABSTRACT This paper presents a comparison of two gain-enhancement techniques and the development of an extremely high-gain slotted waveguide antenna array (SWAA) aiming at applications in the millimeter-waves (mm-waves). The first technique utilizes pairs of grooved structures surrounding a given primary power source to improve its transmission properties, acting as secondary sources to re-radiate the surface wave energy, whereas the second is based on symmetrical wing-based reflectors. Those techniques and their combination have been applied to an SWAA based on an air-filled metallic rectangular waveguide. The proposed antenna array was designed for operation in the frequency range from 25.5 to 26.5 GHz and excited by a unique coaxial-to-waveguide transition with the TE_{10} fundamental mode. These techniques enable us to enhance the gain of the array by up to 10 dB, making it comparable to those of parabolic antennas with similar size apertures. Numerical analyses of the performance-enhanced antenna arrays are presented to validate the design strategies. Experimental results of 27- and 41-slots SWAA prototypes demonstrate the potential of the wing-based reflector technique to improve its aperture efficiency over that of the grooved structures. The 41-slots SWAA prototype provides as high as 31 dBi-gain in the 26 GHz band, ranging from 30.52 to 31.13 dBi within the array impedance bandwidth. Furthermore, since the reflector structures are easily attached to and detached from the SWAA structure, the prototype has the potential to provide both sectoral and directive radiation patterns in the *E*-plane.

INDEX TERMS 5G, antenna, grooved-structures, reflectors and slotted waveguide antenna array.

I. INTRODUCTION

The mobile networks have evolved in response to the system demands for greater capacity and resource-efficient usage. Emerging services and technologies will require flexibility for future Fifth-generation mobile networks, also referred to as 5G [1]–[3]. This network is expected to handle massive device connections per cell related to the massive machine-type communications (mMTC); offering throughput up to 10 Gbps, defining the extreme mobile broadband (eMBB) scenarios; attending to delay-sensitive applications referred to as ultra-reliable low latency (URLL) communications; providing long-range communications for remote area access. These different services and application requirements of the 5G systems have been instrumental in generating the specifications of both the sub-six 450 to 6000 MHz (Frequency Range 1 or FR1) band, as well as the millimeter-wave (mm-wave) band ranging from 24.25 to 52.60 GHz (Frequency Range 2 or FR2) frequency bands for 5G systems [4].

The 5G first networks deployment aims to attend the eMBB services such as broadband Internet access, virtual reality, augmented reality, cloud-based AI, and so forth [3], [5], [6]. These services and applications require high cell throughput, which leads to the FR2 band exploitation since the mm-waves offer unprecedented bandwidth

The associate editor coordinating the review of this manuscript and approving it for publication was Mohammad Zia Ur Rahman.

and worldwide spectrum availability. However, it suffers from a relatively high path loss in comparison to that of the FR1 band, expected since it operates at millimeter-wavelengths [7]. On the other hand, the small wavelength at the mm-waves affords compact antenna array deployment to provide high gain systems and beamforming capabilities. These arrays are often based on microstrip antenna [8], [9], substrate integrated waveguide (SIW) [10]–[12], radial-line slot array antennas (RLSAs) [13]–[18] and slotted waveguide antenna array (SWAAs) technologies [19]–[22].

The following antenna array design aspects play an essential role and should be addressed for developing antenna arrays operating in FR2 [23]–[27]: mutual coupling, low-profile high-gain, and wide-angle beam scanning. Regardless of the array element structure, the radiators are typically relatively close to each other in the near-field region, giving rise to an electromagnetic induction phenomenon, defined as mutual coupling [28]. This phenomenon causes undesirable effects on the array performance and, consequently, on the wireless system. For instance, the antenna array radiation pattern might deteriorate, even due to orthogonal polarization modes excitation, as well as its impedance matching bandwidth [23]. Therefore, lower mutual coupling among the array elements is highly desirable to improve the overall system performance. There are several works devoted to reducing or suppressing mutual coupling, using decoupling networks, parasitic elements, slot etching, defected ground structures, frequency selective surface, metasurfaces, and joining effects of discrete elements and feeding structures [29]–[32].

The aperture antenna array design comprises integrating its excitation with the radiating elements [24]–[26]. Therefore, it could be considered an alternative to conventional high-gain antennas, such as reflector antennas, reflectarrays, and transmitarrays. Notably, we have proposed a low-profile high-gain SWAA based on grooved structures and a simple feeding network [22]. Meanwhile, the beam scanning improvement capabilities are interested in mm-waves antenna array design. However, for scanning angles exceeding 30°, the array suffers from inappropriate gain loss and an increase in the sidelobe level, resulting in the radiation pattern degradation [27]. Those issues have been recently addressed by applying innovative array configurations, which have also exploited our previous publications, to obtain wide-angle scanning antennas for mm-waves 5G applications [22], [27]. Also, researchers have focused on near-field metasurfaces-based transmitarrays to achieve low-profile high-gain radiators with continuous beam-steering by exploiting the metasurface properties [13], [33]–[35]. The designs comprise a primary low-profile high-gain source with a metasurface position on its top in the near-field region to accomplish continuous beam-steering capabilities. The primary source is based on a microstrip antenna, SIW, RLSAs, or SWAAs technologies despite the beam-steering solution.

The microstrip and SIW-based arrays are known to require complex impedance matching networks and/or multiple independent feedings points to excite their elements. For instance, D. Guan *et al*. has proposed a novel 4×4 SIW cavity-backed antenna array without using an individual feeding network that provides 18.8 dBi gain, using 16 slots [12]. This problem is circumvented in the RLSAs and SWAAs design, which has a unique waveguide-to-coaxial transition exciting all their slots milled on the top of a metal plane or into the waveguide walls, respectively. Note that this type of SWAA design comprises directive radiation patterns only in the *H*-plane [19]–[22]. Consequently, to achieve a high-gain structure in the *E*-plane, SWAA-based elements association is a need in the transversal plane, resulting in an array with a complex impedance matching network [36]. Complementary, the current work focuses on exploiting two potential gain-enhancement techniques to design high-gain SWAA while preserving the advantage of a single excitation. The grooved structures, the wing-based reflectors, and their combination are evaluated and applied to achieve a 31-dBi gain SWAA operating in mm-waves. We also aim to provide a prototype with impedance bandwidth higher than 1 GHz, within the New Radio operating band in the FR2 identified as n258 (24.25 to 27.50) [4].

Furthermore, the RLSA radiators comprise positioning radial slots lines to achieve high gain at *E*- and *H*-plane simultaneously [13]–[18]. This solution meets the single feed structures, low-profile and high-gain features persuaded by this work. However, structures and performance metrics drawbacks are observed. The RLSAs rely on waveguides partially filled by dielectric materials, adding manufacturing cost and complexity since some designs require materials with different dielectric constants. In addition, these dielectric materials are lossy and reduce the antenna efficiency, as seen in the broadside directivity and gain presented by the authors in [14], [15]. Regarding the arrangement and number of the slots, we have based on a conventional design with 27- and 41-slots placed along the waveguide longitudinal axis to achieve a 31-dBi array assistant by wing-reflectors. Meanwhile, the RLSAs exploit a large number of slots to achieve similar gains [16]–[18]. It is worth mentioning that the recent designs in [14], [15] do not achieve 30 dBi gain within the impedance bandwidth. Regardless of the arrays wideband performance, the gain is not flat over the impedance bandwidth, which is observed by our design.

It is well-known that reflector structures properly positioned in the vicinity of an antenna can improve its gain by reflecting the electromagnetic wave towards a specific point in the far-field region under constructive interference with the transmission wave [37]. This concept has been numerically applied and evaluated to SWAAs, by symmetrically attaching inclined metal sheets to their structures at the microwave range [38], [39]. Regardless, these microwave designs leak from experimental results while our design meets the mm-wave frequency range operation and has been experimentally validated with superior impedance bandwidth. Moreover, an SWAA using a joint wing-based reflector and a tapered dielectric slab has been proposed for marine

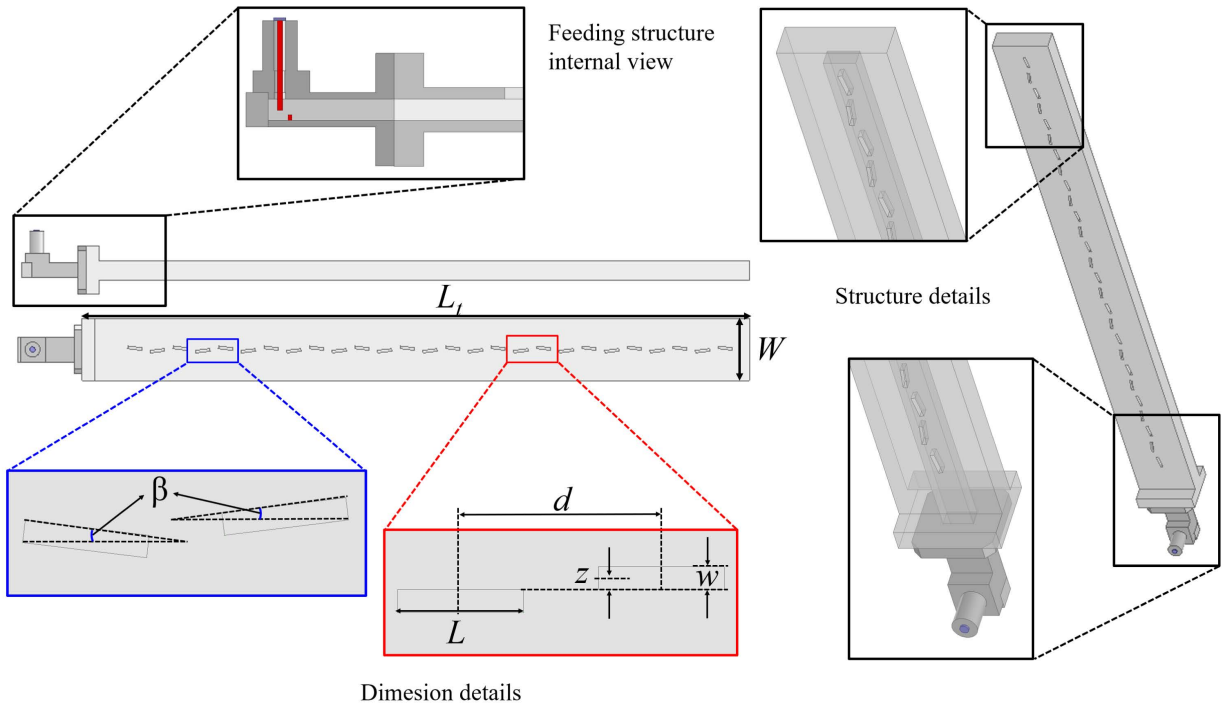

FIGURE 1. SWAA dimension and structure details.

radar applications [40]. The array has performed over the microwave range with lower gain (up to 30 dBi) and efficiency than the wing-based reflector SWAA herein evaluated while showing a complex structure. Some design considers concentrating the radiation by positioning the reflectors vertically [41]. Moreover, a corner reflector has been employed not only to increase the gain of the SWAA but also to control its radiation pattern [42]. The authors in [43] focused on slot displacements techniques to reduce sidelobe level and exploited dielectric slabs at the surface of the slot to achieve a circularly polarized structure.

Metal subwavelength apertures surrounding a given power source have been shown to improve its transmission properties [44], by taking advantage of the fact that grooved structures act as secondary sources and re-radiate the surface wave energy in phase with the primary electromagnetic wave, to realize the improvement in the gain. This is true for grooved-structures whose aperture width is less than the free-space wavelength ($w_r << \lambda_0$), depth (h_r) is approximately equal to an integer multiple $\lambda_0/4$, and distance (d_s) among adjacent structures and primary source around λ_0 [44], [45].

Related works have applied the groove structures to enhance slot antenna gain [46]–[52]. Among these works, Huang *et al*. have numerically analyzed an 8-slot SWAA with 4-pair of groove structures operating at 14 GHz [52]. Recently, the authors have proposed a low-profile and high-gain SWAA operating in the 26 GHz band [22]. Our prototype comprises 27 sloped slots located on the top wall of a standard WR28 waveguide, with 6-pairs of metal grooved structures placed parallel to its longitudinal axis. The bandwidth of the prototype SWAA ranged from 25.88 to 26.78 GHz, and its peak gain was 27.7 dBi, implying that adding the grooved structures resulted in a gain enhancement of 9-dB.

The current work offers two main contributions. First, to the best of our knowledge, it is the first one from the literature that presents a comparison between two efficient gain enhancement techniques, grooved structures and symmetrical wing-based reflectors, including combinations thereof. Second, it reports the development and characterization of a 31 dBi-gain SWAA realized using wing-based reflectors operating in the mm-wave. The manuscript is organized into five sections. Section II presents the basic SWAA model and its main electromagnetic properties. Numerical comparisons of the two gain enhancement techniques are reported in Section III, whereas the prototype and experimental results of the 31 dBi-gain SWAA using wing-based reflectors are outlined in Section IV. Finally, conclusions and final comments are included in Section V.

II. SLOTTED WAVEGUIDE ANTENNA ARRAY DESIGN

SWAAs based on air-filled metallic rectangular waveguides typically provide high-power and high-efficient features since their slots are milled into their broad or narrow walls to provide high-gain, and broadside radiation [19], [22]. The high-gain radiation structure comes with a unique feeding point and an excitation network integrated with the radiators, as seen in Fig. 1. According to the desired radiation mechanism, the SWAAs are grouped in standing or traveling-wave

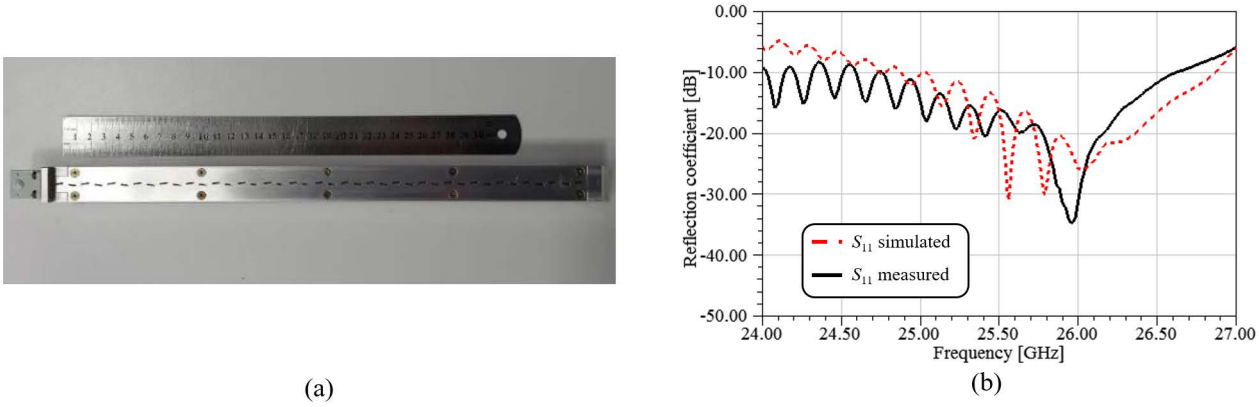

FIGURE 2. SWAA with 41-slop slots. (a) Prototype. (b) Measured and simulated reflection coefficient.

structures. A standing-wave SWAA is obtained by designing a stub-like structure at the waveguide end by placing the last slot center a quarter-wavelength of its end [53]. Additionally, traveling-wave SWAAs present RF loads or absorbing materials to scatter the non-radiated energy. The former is a resonant structure with narrow impedance bandwidth, while the latter operates over a wide frequency range. Regarding the resonant SWAAs, our research group has been devoted to proposing techniques to improve SWAA impedance bandwidth [22], [54], by means of applying groups of slots with different electrical lengths, trapezoidal-shaped slots, twisted distribution of slot groups along the array longitudinal axis and slop slots. The slop slots approach [22] has also been exploited in the current work for developing a resonant air-filled rectangular waveguide SWAA with slots milled into its broad wall.

We follow the design procedure proposed by Elliot in [53] and choose the electrical length (L) equal to 1/2 of the free-space wavelength ($\lambda_0/2$), which is required to guarantee the array resonance at the design frequency. The center-to-center separation distance (d) is equal to 1/2 of the guided wavelength ($\lambda_g/2$) due to the signal propagation inside the waveguide structures. The longitudinal adjacent slots displacement introduces a 180°-phase shift between their radiated electrical fields. Therefore, the slots are moved away from the broadside wall center (z), aiming at a total 360°-phase shift. The first slot center is placed at a quarter of the guided wavelength ($\lambda_g/4$) from the excitation point [53]. This approach is also applied to the last slot near the waveguide end, which results in a stub-like structure. Fig. 1 highlights the arrays main dimensions and structures details, whereas L_t, W, and β are, respectively, the arrays total length, width, and slot inclination. Following our previous work [22], the slots were tilted by 7° to increase the SWAA bandwidth. It is excited by a commercial single waveguide-to-coaxial transition, and its fundamental mode is the TE_{10}. The commercial transition was modeled on the ANSYS HFSS® (Fig. 1) and included in the simulations to enable a rigorous and accurate design.

Fig. 2(a) shows the SWAA design with tilted slots ($\beta = 7°$), with 14 slots added to the previous model so that the total number of slots is now 41. The slot dimensions are as follows: L = 5.55 mm; d = 8.85 mm; z = 0.5 mm; slot width w = 1 mm, L_t = 384 mm, W = 24.1 mm. We choose the ANSYS HFSS®EM simulator to design the antenna array and numerically analyze its performance by using the Finite Element Method (FEM), including the reflection coefficient (S_{11}) displayed in Fig. 2(b). It is observed a good qualitative agreement between the simulated and measured impedance matching results in a fractional bandwidth (FBW) of 7%, from 24.8 to 26.6 GHz, with S_{11} below -10 dB. The simulated and measured results assessment for the SWAA with 27 slots are reported in [22].

III. COMPARISON BETWEEN THE GAIN ENHANCEMENT TECHNIQUES

This section presents the numerical simulations of the designs based on grooved structure and wing-based reflector techniques. The exploited designs are modifications of the SWAA described in the previous section and are depicted in Fig. 3 with the values of the main dimensions best model shown in Table 1. Such arrays are fed by a unique coaxial-to-waveguide transition to avoid mutual coupling from the excitation point of view. However, there is an intrinsic mutual coupling among the array elements, which arises from the higher-order modes (internal mutual coupling) and the presence of the surface waves (external mutual coupling).

Regarding the modifications of the structure, the grooves were symmetrically added to the slot longitudinal direction, as described in our previous publication [22], with a maximum of seven pairs of grooved-structures (Fig. 3(a)). Then, the wing-based reflectors were symmetrically applied to the broadside wall end by considering an inclination angle (α) from 20° to 70° and reflector length (L_w) from 10 to 70 mm (Figure 3(b)). Later, this model was modified by adding up to 3-pairs of grooved-structures, with the same α and L_w, to combine both techniques in a unique array to enhance

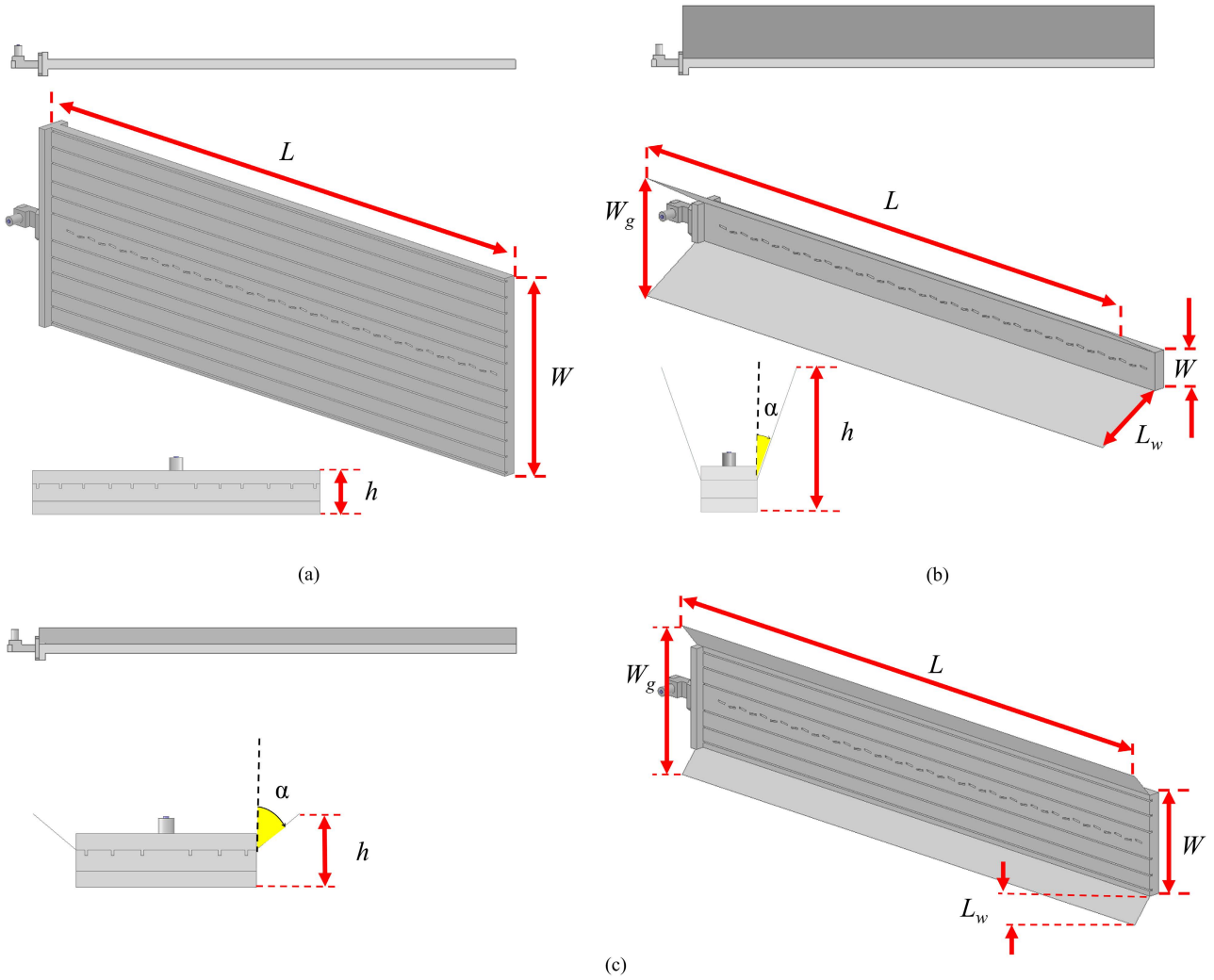

FIGURE 3. High-gain SWAA models. (a) Grooved-structures technique. (b) Wing-based reflector technique. (c) Grooved-structures and wing-based reflectors technique.

TABLE 1. Main dimensions of the 27- and 41-slots SWAAs from Fig 3.

SWAA with 27 slots						
Model	L	W	W_g	h	L_w	α
Grooved-structures only	260mm	124mm	-	19mm	-	-
Wing-based reflector only		24mm	74mm	54mm	50mm	30^o
Wing-base reflector with 03 grooved structures		64mm	96mm			
SWAA with 41 slots						
Model	L	W	W_g	h	L_w	α
Grooved-structures only	384mm	124mm	-	19mm	-	-
Wing-based reflector only		24mm	74mm	51mm	50mm	30^o
Wing-based reflector with 03 grooved structures		64mm	95mm	20mm	20mm	50^o

the gain without compromising their impedance matching performance (Fig. 3(c)). The structures have been evaluated in the range of α and L_w to optimize the gain increment.

Fig. 4(a) presents the gain increment results at 26 GHz, as a function of the number of grooved-structure pairs and wing-based reflector length for the best α. Numerical analyses have been conducted to obtain the α that provides the highest gain increment for each L_w. The grooved structure provided up to 8.14 dB of gain increase with 6-pairs of grooves. The first pair of grooves provides the main contribution to the gain enhancement by 4.91 dB, since the energy level in this region is relatively high, while the other five pairs provide an additional gain of 3.23 dB. Furthermore, the addition of the seventh pair does not provide further

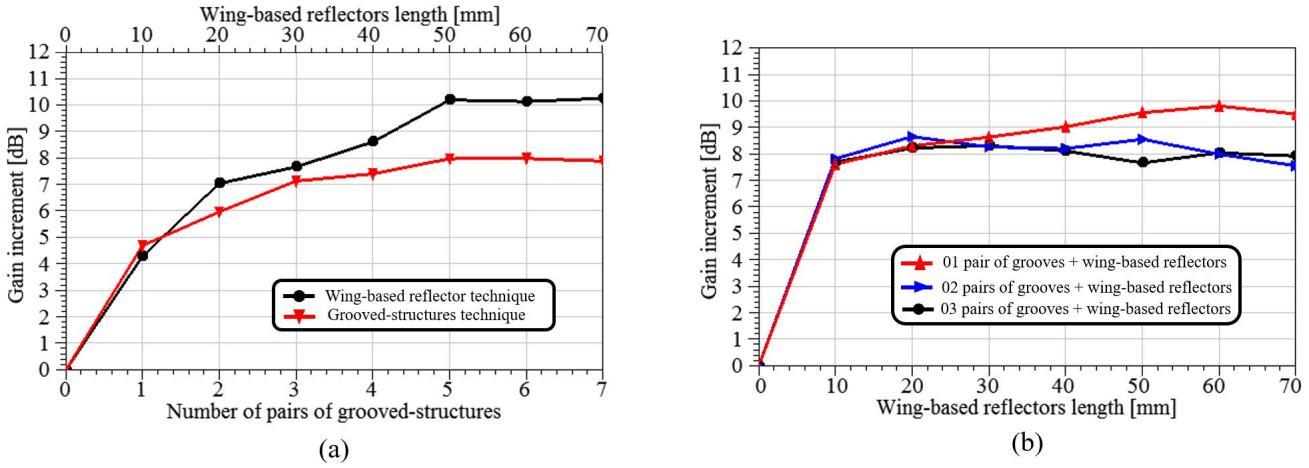

FIGURE 4. (a) Independent analysis of the grooved-structures and wing-based reflector technique gain increment. (b) Simultaneous use of grooved-structures and wing-based reflector.

improvement in the performance. However, attaching the reflector with L_w = 50 mm and α = 30° increases the gain up to 10 dB, although increasing the reflector length has no noticeable effect on the gain of the SWAA. It leads us to conclude that from the point of view of gain enhancement, the wing-based reflector structure is superior to the gain enhancement realized by using the grooves alone since the former provided up to 2 dB additional gain for the cases analyzed.

These results are in agreement with the electromagnetic effects introduced by the structures of each technique surrounding the primary source. The subwavelength grooved structures displaced aside the SWAAs slots introduce a phenomenon that enhances the primary source transmission, which is very similar to the optical wavelengths phenomenon described by the surface plasmons model for metals [44], [45]. The grooves resonate with the slots, reassembly an array in the *E*-plane direction, resulting in the observed gain increment. These transmission enhancement effects rely on the Leaky-Wave Theory, which claims that a surface wave guided through a periodically subwavelength structures surface turns into a leaky wave, partially radiating its energy as it propagates [46], [55], [56]. Since the grooves are seen by the surface wave as resonate cavities, the gain increment comes from the collective excitation of the cavity modes added to the primary source excitation. Moreover, a pair of grooves re-radiates only a fraction of the incoming surface wave energy, introducing the need for a set of groove pairs to enhance the structures overall gain significantly. The remaining surface wave energy level is lower after passing through each pair until reaching a negligible value, which does not effectively contribute to gain increment. This phenomenon is observed in Fig. 4(a) after introducing the 6-pairs under the conducted analysis for an SWAA as aforementioned. Numerical analysis has been employed to find out the α which provides the highest gain increment for each L_w.

Meanwhile, the wing-based reflector works as a corner reflector enhancing the SWAA gain by focusing its beam. The numerical essay has shown that the optimal gain increment occurs to α = 30° for L_w between 40 and 70 mm, while an arbitrary α was observed for values between 10 and 30 mm. The apex angle between the wings-based reflector is an integer sub-multiple of 180° for L_w between 40 and 70 mm, whereas the structures behavior can be described using the electric image theory [57]. Since the angle between the semi-planes equals 60° (each semi-plane is inclined by 30°), the SWAA positioned at the vertex diagonal produce five electric images: $N = (360/2\alpha) - 1 = 5$. Thus, the radiation pattern can be analyzed by applying the array theory, including the SWAA as the real element. Furthermore, the corner reflector well-established theory considers semi-infinite planes under the mathematical models [12], [57]. In practice, the wing-based reflector is truncated, searching for small values that are moderately large related to the source excitation. The analysis provided in Fig. 4(a) has shown a minimum value equal to 50 mm to achieve around 10 dB gain increment. It is worth mentioning that this practical approach leads to back radiation due to the edge diffraction at the end of the reflector.

The next step was to combine both techniques of gain enhancement. We use up to 3-pairs of grooves, the most effective ones with 7 dB gain enhancement, as shown in Fig. 4(b). The performances of the three new models were approximately the same for reflector lengths less than 30 mm, and the gain increase ranged from 7.7 dB (L_w = 10 mm) to 8.6 dB (L_w = 20 and 30 mm). For longer reflector lengths, the model with only 1-pair of the grooves always provided higher gain, achieving up to 9.79 dB of gain improvement. Finally, the wing-based reflector SWAA with $\alpha = 30°$ and $L_w = 50$ mm provided the best gain performance (from 30 to 30.96 dBi over the operating bandwidth). The complexity of this configuration was also the lowest.

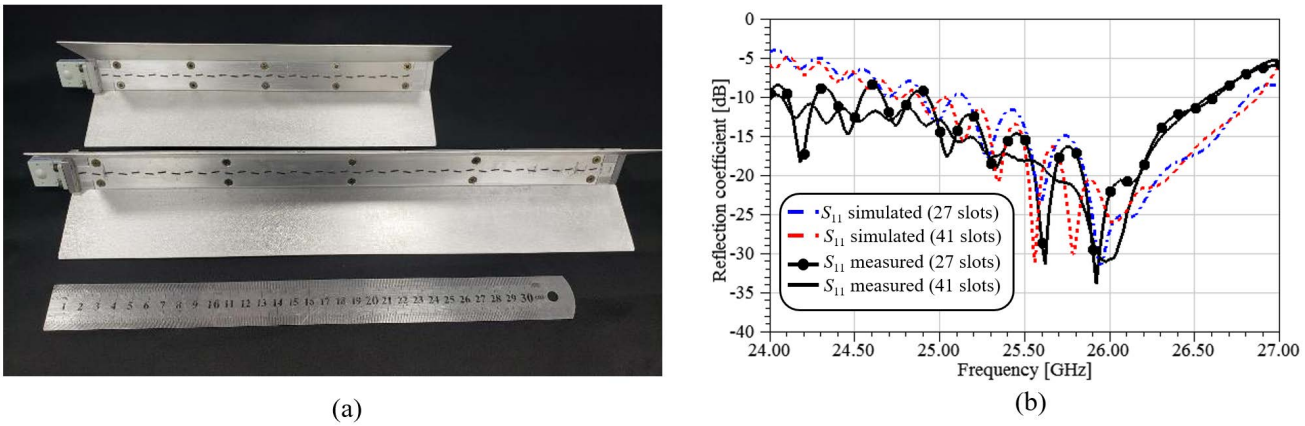

FIGURE 5. SWAA with 27- and 41-slots using wing-based reflectors. (a) Prototypes. (b) Comparison of the magnitude of reflection coefficient.

A parabolic antenna excited by a pyramidal horn antenna, operating in the same frequency band, was designed for the sake of comparison with the proposed SWAA. Relevant design parameters of the reflector are as follows: parabolic reflector diameter D = 172 mm; dish depth D_d = 18.9 mm; feeder length F = 88 mm; horn antenna apertures E_a = 26 mm and H_a = 31 mm; horn antenna peak gain HPG = 11 dBi. The parabolic antenna gain ranges from 30.5 to 30.9 dBi over the frequency range from 25.06 to 26.85 GHz. The SWAA and parabolic antenna weight have been estimated by 3D CAD SOLIDWORKS, considering aluminum alloy 6061. The proposed SWAA final weight was 416.16 grams, which is 6.51% lighter than the parabolic antenna (445.2 grams). It is worthwhile to point out that the SWAA has a superior scan capability in comparison to the parabolic reflector, with the scanning realized by adding phase shifters to the radiating elements of the array.

IV. CHARACTERIZATION OF THE SWAA WITH WING-BASED REFLECTORS

An electro-erosion process was employed to fabricate the 41-slot SWAA with wing-based reflectors, and 1 mm-thickness aluminum bars were used for the process. The resulting inclination angle of the wings was $\alpha = 32°$. Moreover, wing-based reflectors were added to the 27-slots SWAA, whose design may be found in [15]. Fig. 5(a) displays both the 27- and 41-slot versions of the SWAA with wing-based reflectors; add a comparison between the simulated and measured reflection coefficients are presented in Figure 5(b).

The measured FBW for the prototypes with 27- and 41- slots were respectively 6.44% (24.94 to 26.60 GHz) and 9.86% (24.08 to 26.58 GHz). Such bandwidths meet the design requirements while partially covering the n258 operating band in the FR2, allowing 5G applications with a 400 MHz continuous bandwidth operation as specified by standard. In common with the 27-slots prototype from [15], the unexpected occurrence of multiple resonances between 24 and 25 GHz is most likely attributable to the inaccuracies of the fabrication process of the slots, whose lengths were found to vary by approximately 2.9%, between the lowest and highest values, and which in turn resulted in slightly different slot spacing than called for by the design specifications. The 41-slots SWAA prototype provides S_{11} < -15 dB for over 1.2 GHz from 25.1 to 26.3 GHz. Its wider impedance bandwidth comes from the added 14 slots, which extend the waveguide longitudinal length and collaborate to reduce the reflected wave amplitude by radiating an additional fraction of the excitation wave compared with the 27-slots prototype.

The radiation patterns and the gain performance of the SWAA were measured in an indoor environment for the following three frequencies: 25.5, 26 and 26.5 GHz. The measurement setup comprised an analog signal generator (Keysight N5173B) and a 24.7 dBi-gain horn antenna at the transmission side. The proposed array and a spectrum analyzer (Keysight FieldFox N9952A) have been positioned at the reception side. The radiators were mounted at 2 m height and arranged 25 m away from each other to ensure far-field conditions for the lowest measured frequency and highest array dimension. The normalized radiation patterns of the 27-slots SWAA in the H- and E-planes are shown in Fig. 6. A good qualitative agreement is observed, including the null points. The half-power beamwidth (HPBW) in the E-plane has been reduced to approximately 8°, which implies an increased overall array gain. The main lobe tilt in the H-plane radiation pattern at 25.5 GHz (Fig. 6(a)) is related to the slot length (L), and the frequency of the signal applied to the SWAA. Since the frequencies are in the lower limit of the bandwidth, the length of the slot is smaller than that required by design, which slightly tilts the radiation pattern main lobe while increasing the subsequent sidelobe level. However, this level is reduced as the frequency rises within the impedance bandwidth (Fig. 6(b) and (c)).

Table 2 presents the simulated and measured gain results at the frequencies mentioned above, with the measurements

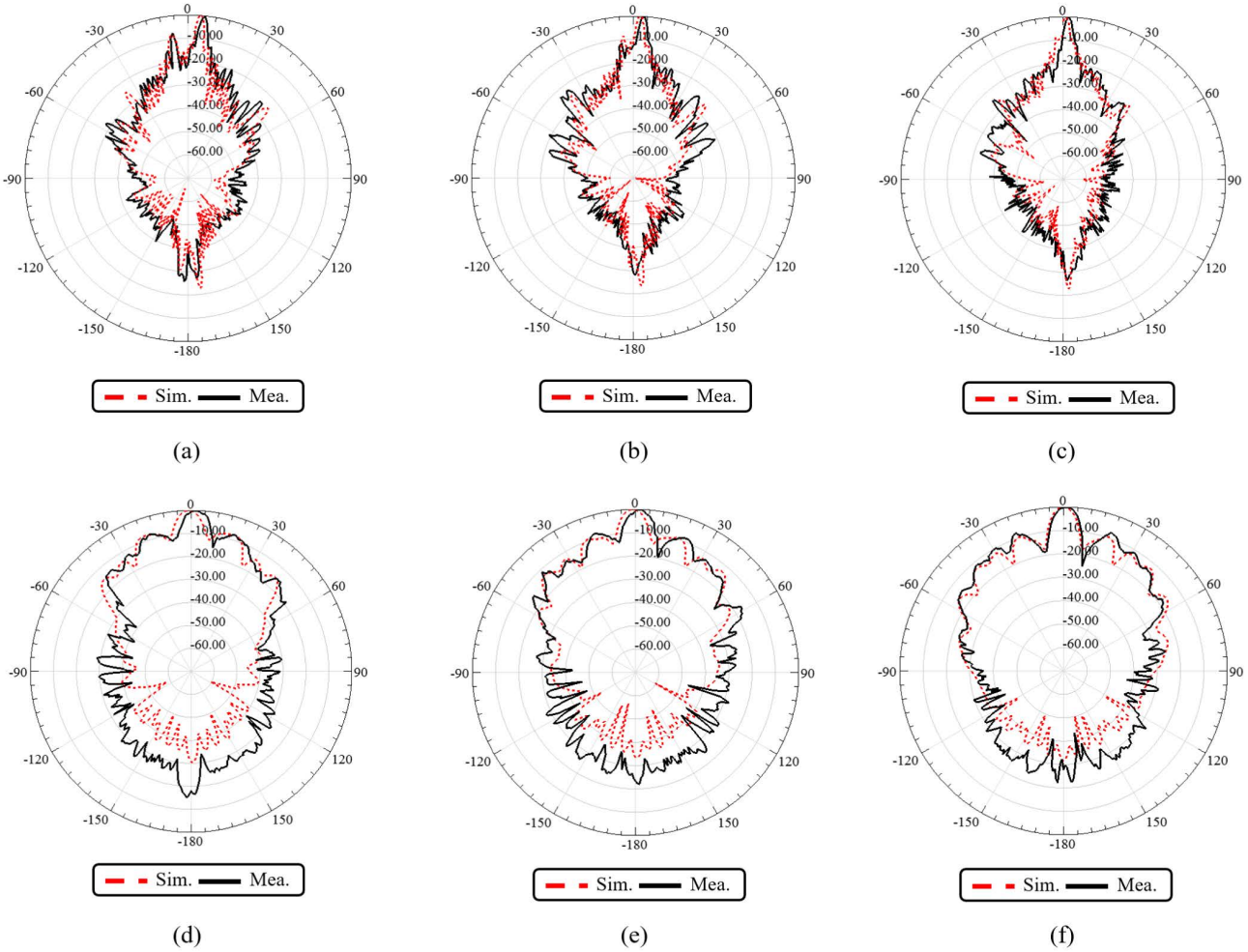

FIGURE 6. Radiation pattern of the 27-slots SWAA with wing-based reflectors (a) *H*-plane at 25.5 GHz, (b) *H*-plane at 26 GHz,(c) *H*-plane at 26.5 GHz,(d) *E*-plane at 25.5 GHz, (e) *E*-plane at 26 GHz, (f) *E*-plane at 26.5 GHz.

TABLE 2. Wing-Based reflectors SWAAs simulated and measured gain.

Freq. [GHz]	SWAA with 27-slots		SWAA with 41-slots	
	Sim. Gain [dBi]	Mea. Gain [dBi]	Sim. Gain [dBi]	Mea. Gain [dBi]
25.5	29.11	29.53	31.06	31.13
26.0	30.03	30.00	31.29	30.06
26.5	29.78	30.09	30.68	30.52

using a 24.7 dBi-gain horn antenna as a reference. The reflectors structures provided a 10-dB gain increase compared with the SWAA without the wing-based reflectors reported in [22]. These results corroborate and validate the numerical results from Section III. Fig 7 reports the gain and radiation efficiency numerical results as a function of frequency for the SWAA with 27- and 41-slots, with and without using wing-based reflectors. A flat gain within the antenna array impedance bandwidth (from 25.5 to 26.5 GHz) is observed for both models. Furthermore, the gain improvement resultant from the use of wing-based reflectors is approximately constant for any analyzed frequency when comparing the results of the 27- and 41-slots SWAAs. The radiation efficiency was above 90% within the impedance bandwidth.

Fig. 8 presents the radiation patterns of the 41-slot SWAA with wing-based slots at the same frequencies as we used before for the 27-slots prototype. Once again, we observe a reasonable qualitative agreement for the main lobes, HPBWs, and nulls. A comparison among the *H*-plane radiation pattern on Fig 6 and Fig 8 has shown that the wing-based reflector improved the front-to-back ratio while significantly reducing the sidelobe levels. Table 2 also includes the gain performances of the prototype. Since the wing-based reflector is array placed, there is no possible arraying at the *E*-plane (i.e., realizing 2D array) for reducing its HPBW and meeting the values obtained at the *H*-plane. However, the HPBW disparity between the planes is lower since their values are 3° and 8°, respectively.

The performance of the prototype has been compared with that of our previous work [22], and with other high-gain

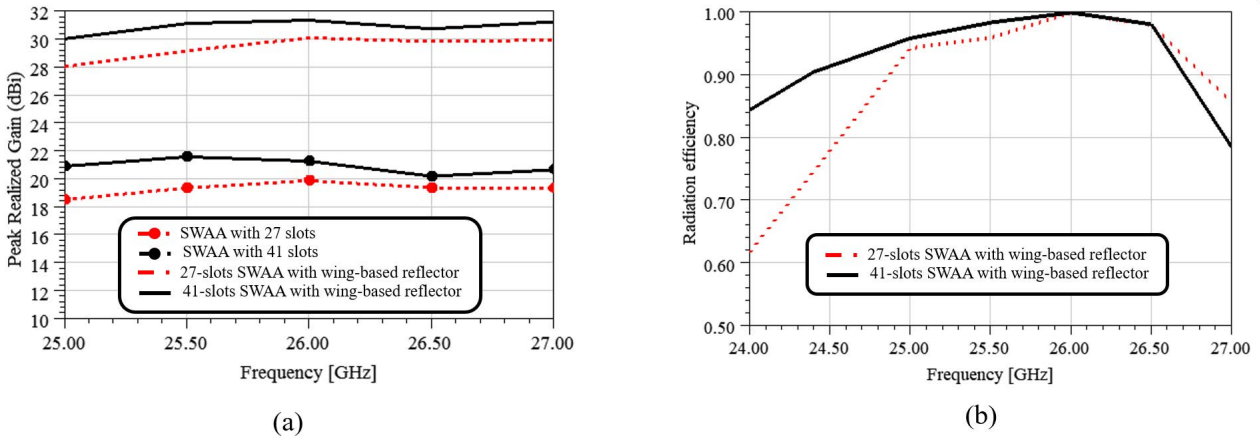

FIGURE 7. (a) Numerical results of the gain as a function of frequency for the SWAA with 27- and 41-slots, with and without using wing-based reflectors (b) Simulated results of the radiation efficiency as a function of frequency for the SWAA with 27- and 41-slots, with wing-based reflectors.

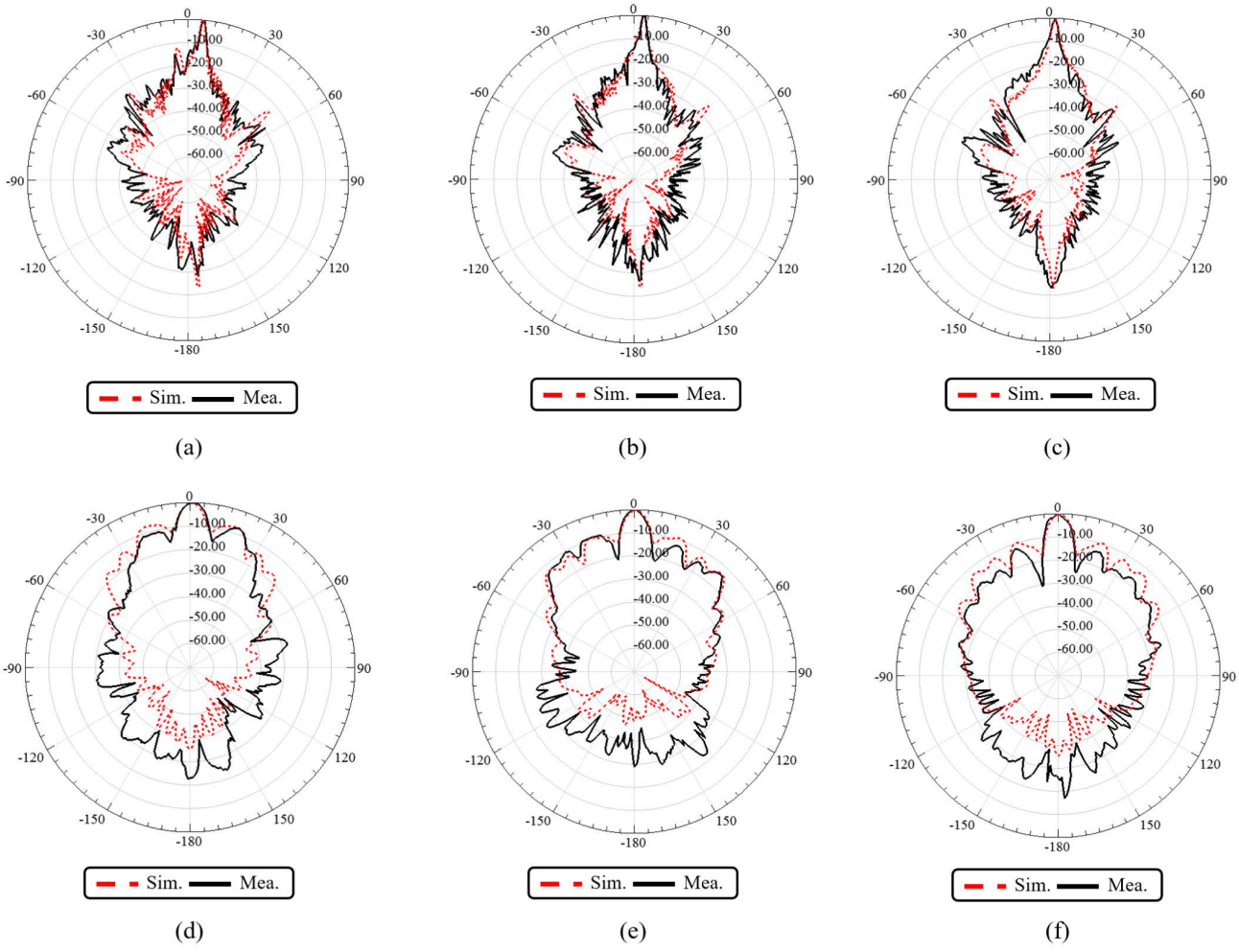

FIGURE 8. Radiation pattern of the 41-slots SWAA with wing-based reflectors (a) *H*-plane at 25.5 GHz, (b) *H*-plane at 26 GHz,(c) *H*-plane at 26.5 GHz, (d) *E*-plane at 25.5 GHz, (e) *E*-plane at 26 GHz, (f) *E*-plane at 26.5 GHz.

antenna arrays based on RLSAs, microstrip antenna, and transmitarrays technology for mm-waves applications [13]–[15], [17], [18], [40], [58]–[62]. Table 3 summarizes the following metrics: array technology, fractional bandwidth,

TABLE 3. Comparison among the proposed antennas with other high-gain antenna arrays.

Ref.	Antenna technology	FBW[%]	Gain [dBi]	SLL [dB]	3dB-gain BW [%]	ϵ_{ap} [%]	Struc. type
This work	Wing-based reflector SWAAA (27 slots)	6.44	30.00	>8.48	6.44	54.00	3D
	Wing-based reflector SWAAA (41 slots)	9.86	31.13	>8.77	9.86	37.80	3D
[13]	Radial-line slot-array antenna	4.97	30.90	>20.00	4.50	22.00	3D
[14]	Radial-line slot-array antenna	34.76	27.30	>7.40	27.60	28.30	2D
[15]	Radial-line slot-array antenna	74.30	28.90	>16.5	6.30	51.00	2D
[17]	Radial-line slot-array antenna	-	27.70	>9	5.78	50.00	2D
[18]	Radial-line slot-array antenna	12.20	33.00	>14	6.80	39.00	2D
[22]	SWAA with grooved structures	3.41	27.70	>11	3.41	20.00	2D
[40]	SWAA with reflectors and tapered dielectric slabs	-	29.4	>12	-	-	3D
[58]	Microstrip antenna array	1.68	27.30	>15	-	59.00	3D
[59]	Microstrip antenna array	10.32	18.70	>15	-	-	3D
[60]	Microstrip antenna array	14.60	25.80	-	-	-	2D
[61]	Microstrip antenna array	-	24.30	>10	-	40.00	2D
[62]	Microstrip antenna array	10.90	21.64	-	-	34.00	2D

gain, sidelobe level (SLL), 3dB-gain bandwidth (BW), aperture efficiency ($\epsilon_{ap} = A_e/A_p$, where A_e is the array effective aperture and A_p is its physical aperture), and structure type.

Regarding our previous work, the tri-dimensional (3D) wing-based reflector SWAAs provide superior performance in comparison to the two-dimensional (2D) SWAA assisted by grooves in terms of FBW, gain (as predicted in Section III), 3dB-gain bandwidth, and aperture efficiency, retaining the simplicity of the excitation system. We observe that we could realize two SWAAs with a significant reduction in the physical array area by easily attaching symmetrical reflectors, achieving aperture efficiencies of 54% and 37.80% for the 27- and 41-slots array, respectively. Notably, the 27-slots SWAA aperture efficiency has overcome the values reported for the RLSAs [13]–[15], [17], [18], being comparable to the array proposed in [58] with a superior gain. Furthermore, the 41-slots SWAA has performed over some RLSAs in terms of aperture efficiency [13], [14], [18] while having provided higher gain than the other designs. Compared to the existing designs, the main advantages of the SWAA design proposed herein are high-gain, simple excitation systems, and low complexity. It is worth mentioning that the reflectors are easily detached from the SWAA structure, resulting in an array with an E-plane radiation pattern directive (with reflectors) or sectoral (without the reflector). This feature enables the design to have dual functionality, rendering it suitable for sectoral or point-to-point applications.

V. CONCLUSION

This work has analyzed the grooved-structures and wing-based reflectors techniques to enhance slotted waveguide antenna array gain. The structures have been individually as well as concurrently added to an SWAA, and their potential for gain improvement has been evaluated for both configurations. Additionally, it has been demonstrated that the wing-based reflectors provide superior performance than the groove-only configuration, with the former achieving 2 dB of additional gain for the best-analyzed cases and a 10-dB increase gain. Two SWAA prototypes with 50 mm wing-based reflectors have been fabricated, and their performances have been compared with that of the legacy SWAA design presented in our previous work [22], which was just a grooved-only structure. It was shown that the 27 and 41-slots SWAAs with wing-based reflectors achieve fractional bandwidth of 6.44% and 9.86, respectively, and up to 31-dBi gain at 26 GHz. Furthermore, the proposed wing-based reflector SWAA enabled a 54% (27 slots) and 37.80% (41 slots) aperture efficiency, which is comparable to that proposed in [36]. Since the reflector structures are easily attached to and detached from the SWAA structure, the prototype has the potential to provide both sectoral and directive radiation patterns in the E-plane.

REFERENCES

[1] P. Popovski, K. F. Trillingsgaard, O. Simeone, and G. Durisi, "5G wireless network slicing for eMBB, URLLC, and mMTC: A communication-theoretic view," *IEEE Access*, vol. 6, pp. 55765–55779, 2018.

[2] R. M. Borges, T. R. R. Marins, M. S. B. Cunha, H. R. D. Filgueiras, I. F. da Costa, R. N. da Silva, D. H. Spadoti, L. L. Mendes, and A. C. Sodré, "Integration of a GFDM-based 5G transceiver in a GPON using radio over fiber technology," *J. Lightw. Technol.*, vol. 36, no. 19, pp. 4468–4477, Oct. 1, 2018.

[3] J. Hwang, L. Nkenyereye, N. Sung, J. Kim, and J. Song, "IoT service slicing and task offloading for edge computing," *IEEE Internet Things J.*, vol. 8, no. 14, pp. 11526–11547, Jul. 2021.

[4] *5G NR, Base Station (BS) Radio Transmission and Reception*, 3GPP, document TS 38.104, 2018.

[5] P. Lin, Q. Song, F. R. Yu, D. Wang, A. Jamalipour, and L. Guo, "Wireless virtual reality in beyond 5G systems with the internet of Intelligence," *IEEE Wireless Commun.*, vol. 28, no. 2, pp. 70–77, Apr. 2021.

[6] T. Zhang, "Toward automated vehicle teleoperation: Vision, opportunities, and challenges," *IEEE Internet Things J.*, vol. 7, no. 12, pp. 11347–11354, Dec. 2020.

[7] T. S. Rappaport, S. Sun, R. Mayzus, H. Zhao, Y. Azar, K. Wang, G. N. Wong, J. K. Schulz, M. Samimi, and F. Gutierrez, "Millimeter wave mobile communications for 5G cellular: It will work!" *IEEE Access*, vol. 1, pp. 335–349, 2013.

[8] Y.-P. Hong, I.-J. Hwang, D.-J. Yun, D.-J. Lee, and I.-H. Lee, "Design of single-layer metasurface filter by conformational space annealing algorithm for 5G mm-wave communications," *IEEE Access*, vol. 9, pp. 29764–29774, 2021.

[9] L. Malviya and P. Gupta, "Millimeter wave high-gain antenna array for wireless applications," *IETE J. Res.*, pp. 1–10, Mar. 2021.

[10] W. El-Halwagy, R. Mirzavand, J. Melzer, M. Hossain, and P. Mousavi, "Investigation of wideband substrate-integrated vertically-polarized electric dipole antenna and arrays for mm-Wave 5G mobile devices," *IEEE Access*, vol. 6, pp. 2145–2157, 2018.

[11] Y. Ding and K. Wu, "A 4 × 4 ridge substrate integrated waveguide (RSIW) slot array antenna," *IEEE Antennas Wireless Propag. Lett.*, vol. 8, pp. 561–564, 2009.
[12] D.-F. Guan, Z.-P. Qian, Y.-S. Zhang, and Y. Cai, "Novel SIW cavity-backed antenna array without using individual feeding network," *IEEE Antennas Wireless Propag. Lett.*, vol. 13, pp. 423–426, 2014.
[13] M. U. Afzal, K. P. Esselle, and M. N. Y. Koli, "A beam-steering solution with highly transmitting hybrid metasurfaces and circularly polarized high-gain radial-line slot array antennas," *IEEE Trans. Antennas Propag.*, vol. 70, no. 1, pp. 365–377, Jan. 2022.
[14] M. N. Y. Koli, M. U. Afzal, and K. P. Esselle, "Significant bandwidth enhancement of radial-line slot array antennas using a radially nonuniform TEM waveguide," *IEEE Trans. Antennas Propag.*, vol. 69, no. 6, pp. 3193–3203, Jun. 2021.
[15] M. N. Y. Koli, M. U. Afzal, K. P. Esselle, and A. Mehta, "Use of narrower reflection-canceling slots to design linearly polarized radial line slot arrays with improved radiation performance," *IEEE Antennas Wireless Propag. Lett.*, vol. 20, no. 12, pp. 2275–2279, Dec. 2021.
[16] M. Albani, A. Mazzinghi, and A. Freni, "Automatic design of CP-RLSA antennas," *IEEE Trans. Antennas Propag.*, vol. 60, no. 12, pp. 5538–5547, Dec. 2012.
[17] J. I. Herranz, A. Valero-Nogueira, F. Vico, and V. M. Rodrigo, "Optimization of beam-tilted linearly polarized radial-line slot-array antennas," *IEEE Antennas Wireless Propag. Lett.*, vol. 9, pp. 1165–1168, 2010.
[18] P. W. Davis and M. E. Bialkowski, "Linearly polarized radial-line slot-array antennas with improved return-loss performance," *IEEE Antennas Propag. Mag.*, vol. 41, no. 1, pp. 52–61, Feb. 1999.
[19] A. C. Sodré, I. F. da Costa, R. A. dos Santos, H. R. D. Filgueiras, and D. H. Spadoti, "Waveguide-based antenna arrays for 5G networks," *Int. J. Antennas Propag.*, vol. 2018, pp. 1–10, Jan. 2018.
[20] E. C. V. Boas, H. R. D. Filgueiras, I. F. da Costa, J. A. J. Ribeiro, and A. C. Sodre, "Dual-band switched-beam antenna array for MIMO systems," *IET Microw., Antennas Propag.*, vol. 14, no. 1, pp. 82–87, Jan. 2020.
[21] H. R. D. Filgueiras, J. R. Kelly, P. Xiao, I. F. da Costa, and A. C. Sodré, "Wideband omnidirectional slotted-waveguide antenna array based on trapezoidal slots," *Int. J. Antennas Propag.*, vol. 2019, pp. 1–8, Oct. 2019.
[22] E. C. V. Boas, R. Mittra, and A. C. Sodre, "A low-profile high-gain slotted waveguide antenna array with grooved structures," *IEEE Antennas Wireless Propag. Lett.*, vol. 19, no. 12, pp. 2107–2111, Dec. 2020.
[23] H. Singh, H. L. Sneha, and R. M. Jha, "Mutual coupling in phased arrays: A review," *Int. J. Antennas Propag.*, vol. 2013, pp. 1–23, Mar. 2013.
[24] W. Hong, K.-H. Baek, Y. Lee, Y. Kim, and S.-T. Ko, "Study and prototyping of practically large-scale mmWave antenna systems for 5G cellular devices," *IEEE Commun. Mag.*, vol. 52, no. 9, pp. 63–69, Sep. 2014.
[25] J. Zhang, X. Ge, Q. Li, M. Guizani, and Y. Zhang, "5G millimeter-wave antenna array: Design and challenges," *IEEE Wireless Commun.*, vol. 24, no. 2, pp. 106–112, Apr. 2017.
[26] G. M. Rebeiz, S.-Y. Kim, O. Inac, W. Shin, O. Gurbuz, Y.-C. Ou, F. Golcuk, T. Kanar, and B.-H. Ku, "Millimeter-wave large-scale phased-arrays for 5G systems," in *IEEE MTT-S Int. Microw. Symp. Dig.*, May 2015, pp. 1–3.
[27] R. Mittra, A. Nasri, and R. K. Arya, "Wide-angle scanning antennas for millimeter-wave 5G applications," *Engineering*, vol. 11, pp. 1–14, Dec. 2021.
[28] J. L. Allen and B. L. Diamond, "Mutual coupling in array antennas," Lincoln Lab., MIT, Cambridge, MA, USA, Tech. Rep. 424 (ESD-TR-66-443), 1966.
[29] M. Alibakhshikenari, F. Babaeian, B. S. Virdee, S. Aïssa, L. Azpilicueta, C. H. See, A. A. Althuwayb, I. Huynen, R. A. Abd-Alhameed, F. Falcone, and E. Limiti, "A comprehensive survey on 'various decoupling mechanisms with focus on metamaterial and metasurface principles applicable to SAR and MIMO antenna systems,"' *IEEE Access*, vol. 8, pp. 192965–193004, 2020.
[30] S. Ebadi and A. Semnani, "Mutual coupling reduction in waveguide-slot-array antennas using electromagnetic bandgap (EBG) structures," *IEEE Antennas Propag. Mag.*, vol. 56, no. 3, pp. 68–79, Jun. 2014.
[31] H. Attia, A. A. Kishk, M. A. Abdalla, S. Gaya, A. Hamza, and A. Mahmoud, "Ridge gap waveguide antenna array with improved mutual isolation for millimeter wave applications," *Int. J. RF Microw. Comput.-Aided Eng.*, vol. 31, no. 11, Nov. 2021, Art. no. e22831.
[32] H. Tat Hui, "Decoupling methods for the mutual coupling effect in antenna arrays: A review," *Recent Patents Eng.*, vol. 1, no. 2, pp. 187–193, Jun. 2007.
[33] M. U. Afzal, A. Lalbakhsh, N. Y. Koli, and K. P. Esselle, "Antenna beam steering by near-field phase transformation: Comparison between phase transforming printed metasurfaces and graded-dielectric plates," in *Proc. Int. Conf. Electromagn. Adv. Appl. (ICEAA)*, Sep. 2019, pp. 0593–0595.
[34] S. Sakurai, J. G. N. Rahmeier, T. Tomura, J. Hirokawa, and S. Gupta, "Millimeter-wave Huygens' transmit arrays based on coupled metallic resonators," *IEEE Trans. Antennas Propag.*, vol. 69, no. 5, pp. 2686–2696, May 2021.
[35] A. Lalbakhsh, M. U. Afzal, T. Hayat, K. P. Esselle, and K. Mandal, "All-metal wideband metasurface for near-field transformation of medium-to-high gain electromagnetic sources," *Sci. Rep.*, vol. 11, no. 1, pp. 1–9, Dec. 2021.
[36] S. S. Seretarov and D. M. Vavriv, "A wideband slotted waveguide antenna array for SAR systems," *Prog. Electromagn. Res.*, vol. 11, pp. 165–176, 2010.
[37] C. A. Balanis, *Antenna Theory: Analysis and Design*, 4th ed. New York, NY, USA: Wiley, 2016.
[38] M. Al-Husseini, A. El-Hajj, and K. Kabalan, "High-gain S-band slotted waveguide antenna arrays with elliptical slots and low sidelobe levels," *Prog. Electromagn. Res.*, vol. 1821, pp. 1–4, 2013.
[39] D. P. Yusuf, F. Y. Zulkifli, and E. T. Rahardjo, "Design of narrow-wall slotted waveguide antenna with V-shaped metal reflector for X-band radar application," in *Proc. Int. Symp. Antennas Propag. (ISAP)*, Oct. 2018, pp. 1–2.
[40] K. Anim, H. A. Diawuo, and Y.-B. Jung, "Compact slotted waveguide antenna array using staircase model of tapered dielectric-inset guide for shipboard marine radar," *Sensors*, vol. 21, no. 14, p. 4745, Jul. 2021.
[41] H. Chu, J.-X. Chen, and Y.-X. Guo, "An efficient gain enhancement approach for 60-GHz antenna using fully integrated vertical metallic walls in LTCC," *IEEE Trans. Antennas Propag.*, vol. 64, no. 10, pp. 4513–4518, Oct. 2016.
[42] M. Milijic and B. Jokanovic, "Design of asymmetrical slot antenna array in corner reflector," in *Proc. 55th Int. Sci. Conf. Inf., Commun. Energy Syst. Technol. (ICEST)*, Sep. 2020, pp. 203–206.
[43] O. Cumurcu, A. Caliskan, Y. E. Yamac, and A. S. Turk, "Design of displaced and circular polarized waveguide slot array antenna with dielectric for K-band radar application," in *Proc. 18th Int. Radar Symp. (IRS)*, Jun. 2017, pp. 1–9.
[44] A. P. Hibbins, J. R. Sambles, and C. R. Lawrence, "Gratingless enhanced microwave transmission through a subwavelength aperture in a thick metal plate," *Appl. Phys. Lett.*, vol. 81, no. 24, pp. 4661–4663, Dec. 2002.
[45] M. Beruete, I. Campillo, J. S. Dolado, J. E. Rodriguez-Seco, E. Perea, and M. Sorolla, "Enhanced microwave transmission and beaming using a subwavelength slot in corrugated plate," *IEEE Antennas Wireless Propag. Lett.*, vol. 3, pp. 328–331, 2004.
[46] M. Beruete, I. Campillo, J. Dolado, J. Rodriguez-Seco, E. Perea, F. Falcone, and M. Sorolla, "Low-profile corrugated feeder antenna," *IEEE Antennas Wireless Propag. Lett.*, vol. 4, pp. 378–380, 2005.
[47] M. Diaz, I. Campillo, J. Dolado, J. Rodriguez-Seco, E. Perea, F. Falcone, and M. Ayza, "Dual-band low-profile corrugated feeder antenna," *IEEE Trans. Antennas Propag.*, vol. 54, no. 2, pp. 340–350, Feb. 2006.
[48] M. Beruete, I. Campillo, J. S. Dolado, J. Rodriguez-Seco, E. Perea, F. Falcone, and M. Sorolla, "Very low profile and dielectric loaded feeder antenna," *IEEE Antennas Wireless Propag. Lett.*, vol. 6, pp. 544–548, 2007.
[49] C. Huang, C. Du, and X. Luo, "A waveguide slit array antenna fabricated with subwavelength periodic grooves," *Appl. Phys. Lett.*, vol. 91, no. 14, Oct. 2007, Art. no. 143512.
[50] X. Gao, S. M. Li, W. P. Cao, Q. Cheng, H. F. Ma, and T. J. Cui, "A highly directive slot antenna with sidewall corrugated structure," *IEEE Antennas Wireless Propag. Lett.*, vol. 12, pp. 1582–1585, 2013.
[51] B. El Jaafari and J.-M. Floch, "Gain enhancement of slot antenna using grooved structure and FSS layer," *Prog. Electromagn. Res. Lett.*, vol. 65, pp. 1–7, 2017.
[52] C. Huang, Z. Zhao, and X. Luo, "The rectangular waveguide board wall slot array antenna integrated with one dimensional subwavelength periodic corrugated grooves and artificially soft surface structure," *J. Infr., Millim., THz Waves*, vol. 30, pp. 357–366, Apr. 2009.
[53] R. Elliott, "An improved design procedure for small arrays of shunt slots," *IEEE Trans. Antennas Propag.*, vol. AP-31, no. 1, pp. 48–53, Jan. 1983.
[54] H. R. D. Filgueiras, E. S. Lima, T. H. Brandao, and A. S. Cerqueira, "5G NR FR2 femtocell coverage map using an omnidirectional twisted SWAA," *IEEE Open J. Antennas Propag.*, vol. 2, pp. 72–78, 2021.
[55] A. A. Oliner and D. R. Jackson, "Leaky surface-plasmon theory for dramatically enhanced transmission through a subwavelength aperture, part I: Basic features," in *IEEE Antennas Propag. Soc. Int. Symp., Dig., Held Conjunct, USNC/CNC/URSI North Amer. Radio Sci. Meeting*, vol. 2, Jun. 2003, pp. 1091–1094.

[56] D. R. Jackson, T. Zhao, J. T. Williams, and A. A. Oliner, "Leaky surface-plasmon theory for dramatically enhanced transmission through a sub-wavelength aperture, part II: Leaky-wave antenna model," in *IEEE Antennas Propag. Soc. Int. Symp., Dig., Held Conjunct, USNC/CNC/URSI North Amer. Radio Sci. Meeting*, vol. 2, Jun. 2003, pp. 1095–1098.
[57] J. A. J. Ribeiro, *Engenharia de Antenas: Fundamentos, Projetos e Aplicações*, 1st ed. São Paulo, Brazil: Érica, São Paulo, 2012.
[58] E. B. Lima, S. A. Matos, J. R. Costa, C. A. Fernandes, and N. J. G. Fonseca, "Circular polarization wide-angle beam steering at Ka-band by in-plane translation of a plate lens antenna," *IEEE Trans. Antennas Propag.*, vol. 63, no. 12, pp. 5443–5455, Dec. 2015.
[59] C. Mao, M. Khalily, P. Xiao, L. Zhang, and R. Tafazolli, "High-gain phased array antenna with endfire radiation for 26 GHz wide-beam-scanning applications," *IEEE Trans. Antennas Propag.*, vol. 69, no. 5, pp. 3015–3020, May 2021.
[60] B. Feng, Y. Tu, J. Chen, S. Yin, and K. L. Chung, "Dual linearly-polarized antenna array with high gain and high isolation for 5G millimeter-wave applications," *IEEE Access*, vol. 8, pp. 82471–82480, 2020.
[61] P.-Y. Feng, S.-W. Qu, X.-H. Chen, and S. Yang, "Low-profile high-gain and wide-angle beam scanning phased transmitarray antennas," *IEEE Access*, vol. 8, pp. 34276–34285, 2020.
[62] Y. Liu, A. Zhang, Z. Xu, S. Xia, and H. Shi, "Wideband and low-profile transmitarray antenna using transmissive metasurface," *J. Appl. Phys.*, vol. 125, no. 4, Jan. 2019, Art. no. 045103.

EVANDRO C. VILAS BOAS received the B.Sc. degree in telecommunication engineering and the M.Sc. degree from the National Institute of Telecommunications (Inatel), in 2016 and 2019, respectively. He is currently a Postdoctoral Fellow at Inatel and an Engineering Researcher with the Wireless and Optical Convergent Access Laboratory (WOCA Laboratory). He also works with the Cyber Security and Internet of Things Laboratory (CS&I Laboratory) supervising undergraduate students in research projects related to the Internet of Things, software-defined radio, artificial intelligence applied to telecommunications research projects, and team guidance in the area of IoT and nanosatellite (CubeSat and CanSats). He has joined the National Institute of Telecommunication as an Auxiliary Professor. He has experience and interests in radio frequency, antennas, propagation, the Internet of Things, mobile communication networks, and software-defined radio.

MARCO A. S. FERRERO received the B.Eng. degree in electrical and electronic engineering from the Instituto Nacional de Telecomunicações—Inatel, Brazil, in 2010. He is currently pursuing the M.Sc. degree with the Wireless and Optical Convergent Access Laboratory, Instituto Nacional de Telecomunicações. His expertise working on Defense and Telecommunication Industry as a RF Development Engineer. His research interests include the design of mmWave devices for LTE and 5G NR applications, such as printed filters, antenna array and phase shifters, and channel estimation using modeling and full wave simulation in digital massive MIMO applications.

ABDELKHALEK NASRI received the B.Sc. degree in electronic systems and the Ph.D. degree in electronics from the Science Faculty of Tunis, Tunisia, in 2011 and 2017, respectively. Actually, he is currently a Postdoctoral Fellow with the Electrical and Computer Engineering Department, University of Central Florida, Orlando, FL, USA. His research interests include high gain phased arrays, frequency selective surfaces, substrate integrated waveguides, scattering of electromagnetic waves, and computational electromagnetics.

RAJ MITTRA (Life Fellow, IEEE) is currently a Professor with the Electrical and Computer Engineering Department, University of Central Florida (UCF), Orlando, FL, USA, where he is also the Director of the Electromagnetic Communication Laboratory. He also holds an appointment at Pennsylvania State University, University Park, PA, USA. Prior to joining Penn State, he was a Professor in electrical and computer engineering with the University of Illinois Urbana–Champaign, from 1957 to 1996. He is also a Past-President of AP-S, and he has served as an Editor of the IEEE TRANSACTIONS ON ANTENNAS AND PROPAGATION SOCIETY. He is currently the Editor-in-Chief of FERMAT, an e-journal published by the UCF with the endorsement of the IEEE/AP Education Society. He has received numerous awards and medals from the IEEE, and from the AP Society. He was recently recognized for his contributions by the URSI with the Rawer Medal, and the Alexander Graham Bell Award from the IEEE Foundation. He is the Principal Scientist and the President of RM Associates, a consulting company founded in 1980, which provides services to industrial and governmental organizations, both in U.S. and abroad. A partial list of his recent publications may be found via Google Scholar Search.

ARISMAR C. SODRÉ, JR. received the B.Sc. degree in electrical engineering from the Federal University of Bahia, Brazil, in 2001, the M.Sc. degree from the State University of Campinas (Unicamp), Brazil, in 2002, and the Ph.D. degree from Scuola Superiore Sant'Anna, Italy, in 2006. He was an Invited Researcher and a Professor at many world-recognized universities, such as the University of Oulu, in 2017, Scuola Superiore Sant'Anna, Italy, in 2015 and 2017, Danish Technical University, Denmark, in 2013, the Max-Planck Institute, Germany, in 2010, and the University of Bath, U.K., in 2004, 2005, and 2007. Since 2009, he has been acting as a Coordinator of Research and Development Projects on diverse areas of telecommunications, including antennas, 5G networks, radars, and microwave photonics. He was an Associate Professor with Unicamp, from March 2009 to August 2011. Then, he joined the National Institute of Telecommunications, Brazil, as an Associate Professor. He holds ten patents, has transferred 25 products to the industry, and has published over 300 scientific papers.